



PERGAMON

Building and Environment 36 (2001) 1–14

BUILDING AND
ENVIRONMENT

www.elsevier.com/locate/buildenv

Location of air intakes to avoid contamination of indoor air: a wind tunnel investigation

N.E. Green*, D.W. Etheridge, S.B. Riffat

The Institute of Building Technology, The School of the Built Environment, The University of Nottingham, Nottingham NG7 2RD, UK

Received 14 September 1998; received in revised form 17 May 1999; accepted 7 September 1999

Abstract

The location of air intakes is of prime importance in buildings that are situated in close proximity to busy urban roads. If intakes are placed where the concentration of traffic pollution is high then indoor air concentrations can reach similarly high levels. This paper presents the findings from a wind tunnel investigation into the dispersion of a simulated traffic pollutant in a 1:100 scale model. The concentrations at different points on a building in the model are measured and a comparison with full-scale data is made. © 2000 Elsevier Science Ltd. All rights reserved.

1. Introduction

Traffic pollution is of increasing concern in many of the world's cities. Occupants in buildings situated close to busy roads can expect to be exposed to a range of pollutants emitted by the motor vehicle such as oxides of nitrogen, volatile organic compounds and carbon monoxide (CO). Although the health effects of these pollutants are not yet fully understood, asthma, other respiratory diseases and some cancers have all been linked to traffic emissions [1,2]. On an urban scale, 89% of all the carbon monoxide in the atmosphere is due to the motor vehicle [3] and the concentration of CO in the atmosphere has been shown to be a good indicator of the concentration of other traffic related contaminants [4].

Wind tunnel modelling of the atmospheric boundary layer has been extensively used in the past to predict pollutant concentrations around buildings as a result of a pollution incident — such as the discharge of effluent from an adjacent stack or the exhaust from motor vehicles at a nearby road junction. Wind tunnels allow the complex airflow patterns that develop around structures to be modelled and are an important

tool in the study of the dispersion and transport of traffic pollutants in the urban environment. When concentration measurements are taken in the field there is no control of parameters such as wind speed, wind direction and ambient temperature and as a consequence the interpretation of data is often difficult. A wind tunnel not only offers control over these parameters but also facilitates a more efficient and economical testing regime.

Previous studies of pollutant dispersion around scale models in wind tunnels can to a large extent be categorised into one of three forms: (i) an idealised city; (ii) a single building with simplified geometry; and (iii) a site specific problem. In most studies, an inert tracer gas such as sulphur hexafluoride (SF₆), ethane or krypton 85 is injected at specific points in the model to simulate the pollutant source (i.e. traffic exhaust) and concentration measurements are then taken at different points on the model for a range of wind directions. Dispersion studies of idealised city forms have illustrated the interaction of the geometry of the urban environment and wind conditions in determining the dilution of traffic pollution. In these studies the simplified city is typically modelled as an orthogonal grid of streets and avenues with a stationary traffic queue modelled as a line of discreet emission points [5–7].

* Corresponding author.

Nomenclature

C_1 concentration at location 1 (ppm)
 C_2 concentration at location 2 (ppm)
 d displacement height (m)
 K concentration coefficient
 K_L model length scale
 k von Karman's constant (0.4)
 M emission rate (g/s)
 Q volume flow rate of air (m^3/s)
 U^* friction velocity (m/s)

$U_{(z)}$ mean velocity at height z (m/s)
 z height above datum (m)
 $z_{(0)}$ roughness length (m)
 Re building Reynolds number

subscripts p and m denote model and prototype and concentrations are expressed in volumetric parts per million (ppm)

Model studies of pollutant dispersal around single buildings have highlighted the significance of flows in the wake of buildings in determining the pollution concentration [8,9]. Wake flows were found to be heavily dependent on the building shape and orientation and on the scale of the approaching boundary layer.

If the correct scaling conditions are applied to a model, then wind tunnel measurements of pollutants around even complex buildings can be representative of those found in the field. This was illustrated in a site-specific study in which the dispersion of gases in a built up area were investigated to assess the impact of an accidental release of a toxic gas at an industrial plant [10]. Wind tunnel results were compared to measurements obtained in the field and in general the data indicated excellent agreement. In a further validation of field and wind tunnel measurements, it was shown that the dispersion of exhausts from motorways could be adequately simulated in a wind tunnel since the wind turbulence causing the dispersion depended primarily on the geometry of the surroundings [11].

When considering the ventilation of a building in the urban environment, either by natural or mechanical methods, the position of openings/air inlets is of great importance if the contamination of the indoor air is to be avoided [12,13]. Studies have shown that if openings are placed where the pollutant concentration is high then indoor concentrations can reach similarly high levels [14,15]. Wind tunnel studies can therefore be very useful in providing information on where best to locate air inlets. Previously, few studies have used wind tunnel measurements in this way to assess the impact of different vent locations. A notable exception to this was a study used to evaluate odour problems associated with diesel trucks at loading docks. In this study the effects of different air intake locations and building configurations were investigated [16].

The current study is concerned with the concentration of traffic pollutants at the facade of a naturally ventilated building situated in close proximity to a busy urban ring road. Tracer gas concentrations were measured on a 1:100 scale model and compared to car-

bon monoxide levels obtained in a previous field study [17]. The results are then used to evaluate different air intake positions.

2. Wind tunnel testing

2.1. Low velocity atmospheric wind tunnel

The wind tunnel used in the tests was a small open-jet wind tunnel capable of delivering a maximum air speed of 4.5 m/s. The working section has a width of 1 m, height 0.75 m and length 2.25 m [18]. The wind tunnel is relatively simple, and its use may be criticised on the grounds that it does not allow appropriate simulation of the turbulence structure. The mean velocity can be reasonably well simulated, but there is no real control over the generation of turbulence. In particular, the small upstream fetch and the relatively large size of the model (compared to the tunnel dimensions) do not allow for artificial generation of large-scale turbulence in the outer boundary layer, nor small-scale turbulence close to the ground.

The choice of model scale factor ($K_L = 100$) is based on practical convenience rather than the scales of turbulence, although as noted in Section 2.2, there is evidence from the mean velocity profile that the small-scale turbulence is reasonably simulated; this may be misleading because the mean velocity and the turbulence are unlikely to be in equilibrium with such a small fetch. On the positive side, there is some evidence that the importance of turbulence generated in the proximity of the building has been underrated in the past [19].

There are also other arguments for at least attempting to use such a simple tunnel for the present purpose. First, it is an inexpensive facility in terms of capital and running costs. This can be an important factor when dealing with the design of buildings for which the development budgets are often likely to be small.

On a more technical level, for ventilation design purposes it is not absolute values that are of prime interest, but relative values. The objective here is to determine the best positions for air inlets. The absolute values will depend on the emission rates that are outside the control of the designer. Furthermore, it is mean values that are of interest, rather than instantaneous values or levels of fluctuation. This is simply due to the fact that indoor concentrations take a finite time to build up. If the mean concentration at an opening is simulated, but the fluctuations are not, the resulting error in indoor concentrations is likely to be small unless there is a strong correlation between the concentration and the flow rate at the opening [20]. On this basis the simulation of turbulence structure is less important than it is, say, for the design of structures where instantaneous gust loading is of prime concern. Of course turbulence levels do affect the mean values, such as mean concentrations in the dispersion

of plumes. However such effects will be reduced in the present tests by the virtue of the fact that we are not dealing with a point emission source, but one which approximates to a two-dimensional line source.

2.2. Non-uniform velocity profile

At the end of the settling chamber, a grid of horizontal slats is used to generate a non-uniform velocity profile in the tunnel. A staggered arrangement of 70 mm cubes was placed 450 mm downwind of the slats to represent the low urban environment in the immediate vicinity of the modelled area. The variation of mean longitudinal velocity with height in the tunnel is represented by the logarithmic velocity profile for a thermally neutral atmosphere, i.e.:

$$U(z) = \frac{U^*}{k} \ln \left[\frac{z-d}{z_0} \right] \tag{1}$$

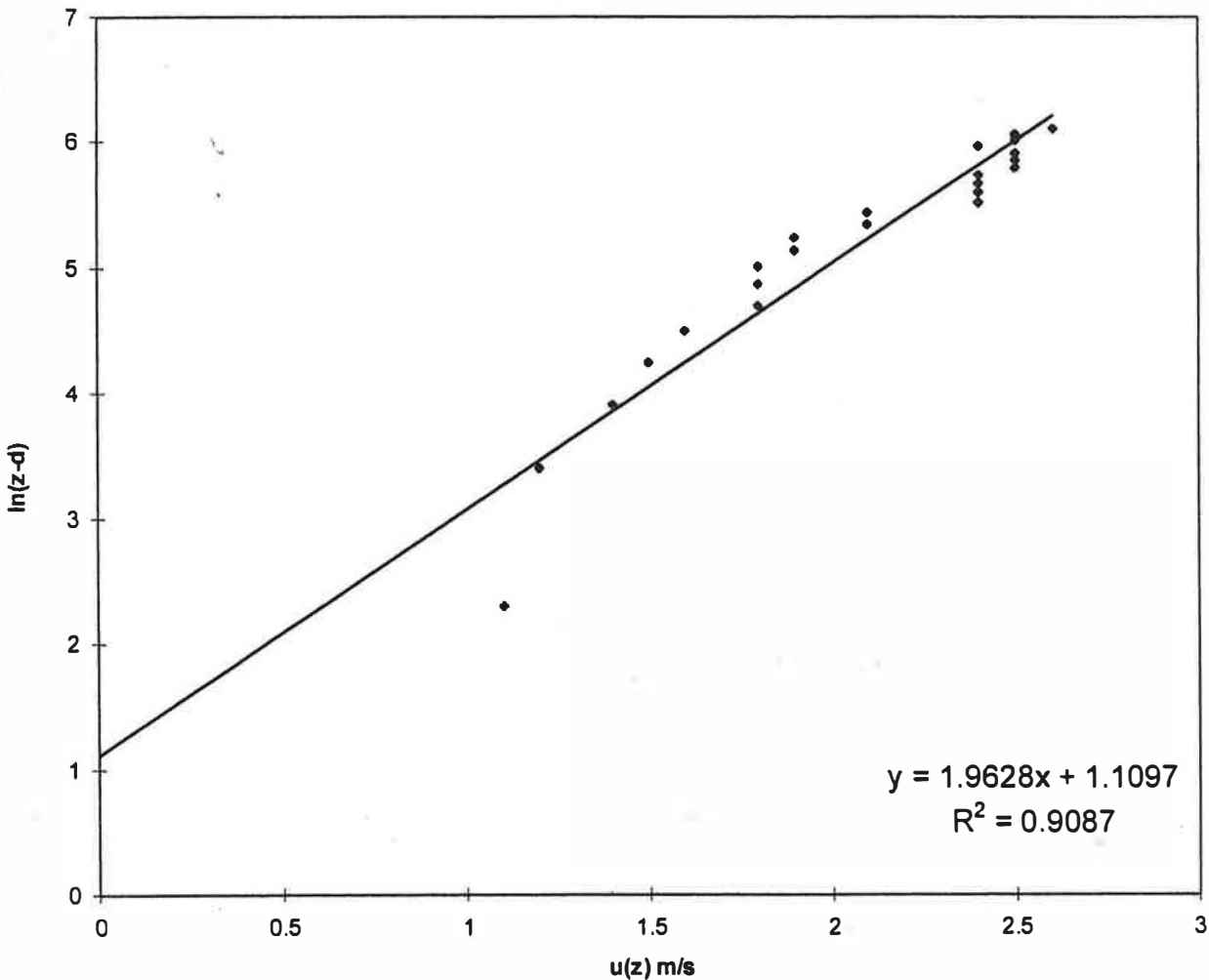


Fig. 1. Wind tunnel logarithmic velocity profile.

rearranging Eq. (1) gives:

$$\ln(z-d) = \left(\frac{k}{U^*}\right)U_{(z)} + \ln(z_0) \quad (2)$$

Fig. 1 shows a plot of $U_{(z)}$ vs $\ln(z-d)$ for a reference wind velocity in the tunnel of 2 m/s and displacement height of 70 mm (i.e. the height of the cubes). The velocity profile was measured using a Pitot tube placed at

the edge of the model. From Fig. 1 the y -intercept, $\ln(z_0)$, is equal to 1.11 giving a value for z_0 of 3.0 mm. Although the measurements are relatively crude, the equivalent full-scale value of z_0 is 0.3 m, which is reasonably representative of the area under consideration. Typically a value for z_0 of between 0.3 and 0.4 m would indicate terrain similar to the outskirts of town, a few kilometres upwind of the site, whilst a value

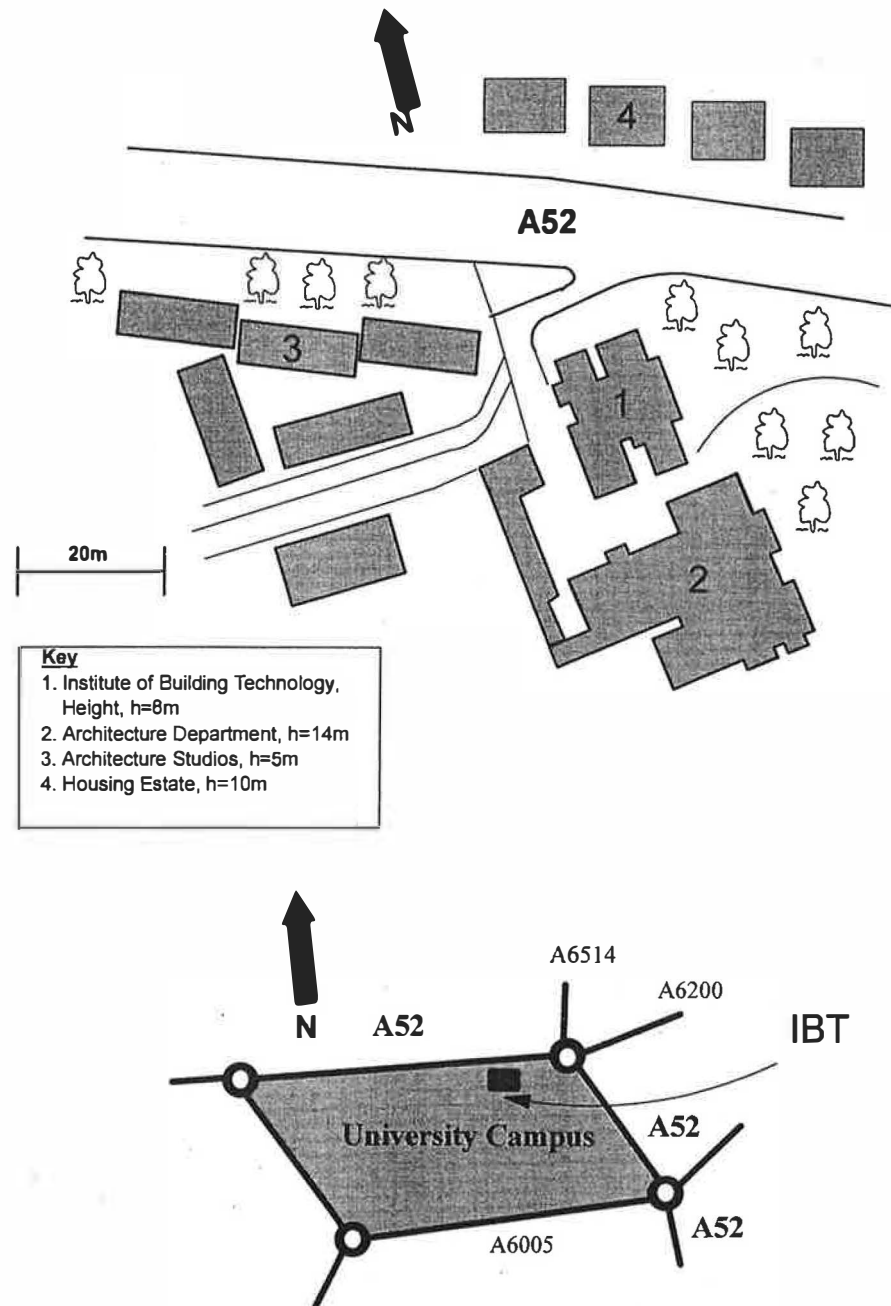


Fig. 2. Area modelled in the wind tunnel and the position of the IBT relative to the local road network.

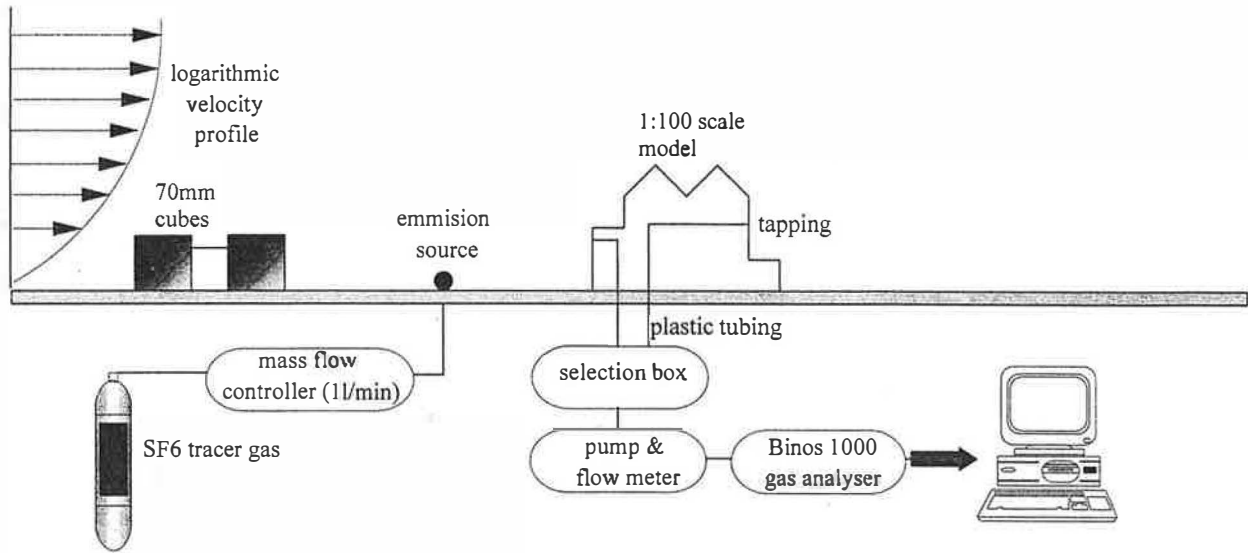


Fig. 3. Wind tunnel set up and apparatus.

between 0.4 and 1.0 m would represent the centre of a small town [21].

2.3. Reynolds number (Re)

For sharp-edged (bluff-body) buildings, the flow field should be independent of the approach velocity if the Reynolds number, Re , is greater than a critical value (typically quoted as 11,000). With a reference tunnel speed of 2 m/s and a characteristic model length of 8 cm (building height), the value of Re is 1.3×10^4 — i.e. greater than the critical value.

3. Scale model construction

A 1:100 scale model was constructed of the area shown in Fig. 2. The Institute of Building Technology (IBT) is housed in a naturally ventilated building situated in close proximity to a busy urban ring road (A52). Traffic flow figures supplied by Nottinghamshire County Council for this section of the A52 show that rush-hour peak flows are typically in the region of 2500 vehicles per hour in each direction. During these peak periods traffic can be stationary for short periods, whilst at other times the traffic is to a large extent free flowing. Total daily flows are in the region of 25,000 vehicles in each direction.

The model of the IBT building was constructed from 3 mm perspex and the surrounding buildings and features constructed from medium-density fibreboard. Prior to making the model, a surveying exercise was performed to determine the gradient of the road and the relative height of the IBT with respect to the road; this detail was incorporated into the model. It was

necessary to simplify some of the finer architectural detail on the buildings due to the scale of the model and no attempt was made to model any surface roughness.

To simulate the exhaust emitted from a queue of stationary traffic, 40×1 mm diameter holes were drilled in a 800 mm length of 9 mm internal diameter copper tubing. The holes were separated by 20 mm to represent an average spacing of 2 m full scale between successive vehicle exhausts in congested traffic. The tube was then positioned on the model at the centre line of the roadway. SF_6 tracer gas was delivered to the tube at a controlled rate of 1 l/min via a Bronkurst mass flow controller.

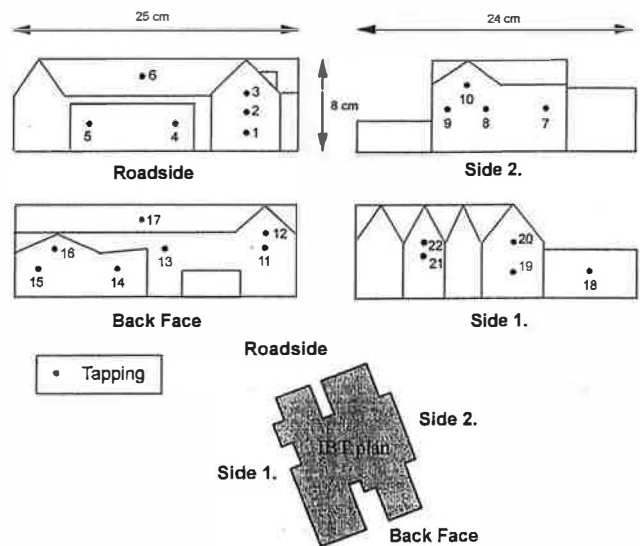


Fig. 4. Location of the tappings on the 1:100 scale model.

The IBT model was fitted with several tapplings (0.8 ID mm brass tubing) flush on its surface to allow measurement of tracer gas concentration at different locations. Plastic tubing was attached to each of the tapplings via a hole in the wind tunnel table and connected to the instrumentation as shown in Fig. 3.

In total, 20 different sampling locations were selected on four of the building faces and, in addition, two tapplings were placed on the roof (Fig. 4). Table 1 shows the heights of each tapping on the model. Analysis of the gas samples was carried out using a Binos 1000 gas analyser connected to the tapplings via a selection box and the concentrations recorded directly onto a personnel computer running a simple logging programme. On a weekly basis the span and zero point of the gas analyser were calibrated using a standard gas. Drift was found to be within $\pm 5\%$.

4. Experimental procedure

The concentration of SF₆ was measured at each tapping for nine different wind angles and a constant reference velocity of 2 m/s measured at 0.6 m above the wind tunnel table. Due to limitations in the logging program it was only possible to log concentrations every second, so for each location readings were taken over a period of 1 min (i.e. 60 readings) and an average calculated. The selection box was manually adjusted between successive locations and since this involved entering the tunnel a 2-min period was

Table 1
Tapping heights on 1:100 scale model

Tapping	Height (cm)
1	1.5
2	3.5
3	5.5
4	3.5
5	3.5
6	7.0
7	3.5
8	3.5
9	3.5
10	5.5
11	3.5
12	5.5
13	3.5
14	2.0
15	2.0
16	3.5
17	7.0
18	2.0
19	2.0
20	5.5
21	3.5
22	5.5

Table 2

Maximum concentrations of tracer gas measured in the wind tunnel at the roadside and back face for different wind directions

Wind direction	Maximum tracer gas concentration roadside face		Maximum tracer gas concentration back face		Percentage reduction between roadside and back face
	ppm	tapping	ppm	tapping	
West	< 5	All	< 5	All	Nil
N West	< 5	All	< 5	All	Nil
NN West	180	5	45	5,12	75
North	340	1	170	16	50
NN East	220	4	65	15	70
N East	160	4	120	12	25
EN East	185	5	170	14	10
East	215	4	65	12	70
S East	< 5	All	< 5	All	Nil

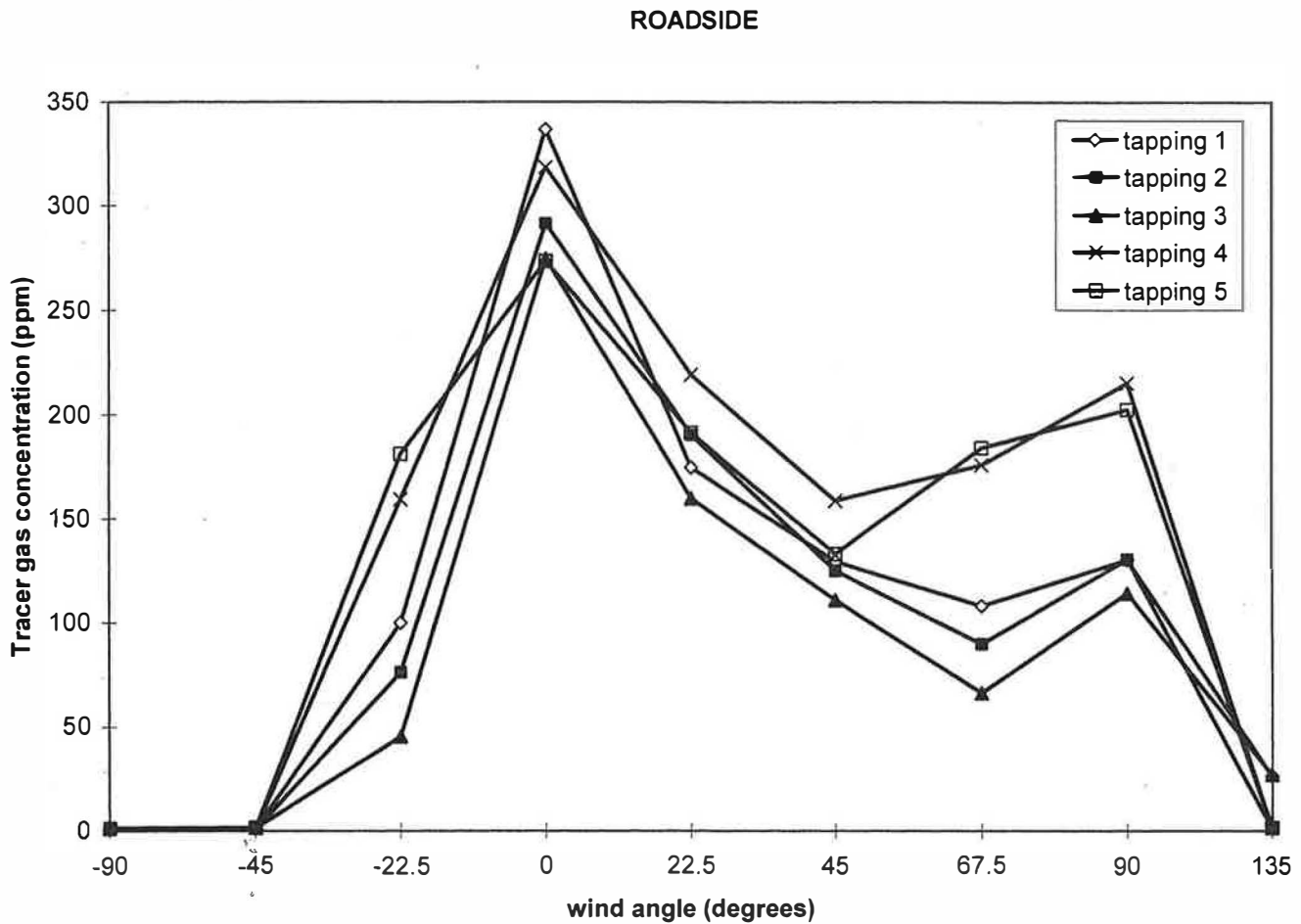


Fig. 5. Tracer gas concentrations (ppm SF₆) recorded at the roadside tappings in the windtunnel. 0 deg=North wind.

allowed between runs to enable the flow field to stabilise.

5. Wind tunnel test results

The average concentration recorded at each location for the different wind directions is shown in Figs. 5–8. It is evident that for most of the tappings the highest concentration occurs when the wind is from a northerly direction (i.e. the building is downwind of the pollutant source) and that the concentrations are greatest on the roadside face. The maximum concentrations on Side 1 are comparable to those on the roadside face and those on Side 2 similar to the back face.

5.1. Concentrations at the roadside and back face

Table 2 shows the maximum concentrations recorded at the roadside and back face for different wind directions. The maximum concentrations on the roadside and back face occur when the wind is from the north, i.e. 340 ppm at tapping 1 and 170 ppm at

tapping 16. This represents a reduction of 50% between the maximum at the roadside and back face. With different wind directions, reductions of up to 75% were observed between the roadside and back face maxima.

5.2. Variation in concentration with height

The variation in tracer gas concentration with height was also considered. Taking the north wind case, Table 3 shows the difference in concentration with

Table 3
Variation in measured tracer gas concentration with height on the roadside face

Tapping	Height (cm)	Average tracer gas concentration (ppm)
1	1.5	340
2	3.5	290
3	5.5	270
4	3.0	320
5	3.0	270
6 (roof)	7.0	110

height on the roadside face. Tappings 2 and 3 on the model represent the position of the ground and first-floor windows on the full-scale building. Under steady state conditions there is a reduction of 7% between the concentration recorded at the ground floor window and that recorded at the first floor.

5.3. Concentrations at roof level

A tapping was placed on the roof of the model at a height of 7 cm, on both the roadside and back face. From Fig. 9 it can be seen that the tracer gas concentration at both roof top tappings was highest when the wind was from the north. In this case, a maximum concentration of 110 ppm was recorded at the roadside roof tapping, which represents a reduction of almost 70% in the maximum concentration recorded on the roadside wall (340 ppm at tapping 1), and a reduction of 60% from the concentration recorded at tapping 2 (ground floor window). Slightly greater reductions were found at the back face roof tapping, 75% and 70% respectively.

6. Comparison of wind tunnel and field measurements

In two separate experiments field-data was collected around the area modelled in the wind tunnel study. In the first experiment (Experiment 1), CO concentrations were recorded at 15 min intervals over a two-week period at the kerbside of the A52, and at a ground-floor window on the IBT building (equivalent to tapping 2 on the model). In the second experiment (Experiment 2), an additional sample point was added at a first floor window (equivalent to tapping 3 on the model). Local wind direction and velocity were recorded in Experiment 1 by means of a wind vane mounted on the roof of the IBT building.

Table 4 summarises the results from the field study. The lower average concentrations recorded in the second week of Experiment 1 were a result of the different wind conditions experienced. In the first week the average wind direction was such that the IBT was downwind of the traffic source (i.e. between northerly and southerly), whilst in the second week the average wind direction was such that the IBT was upwind of the traffic source. The dilution in CO concentration

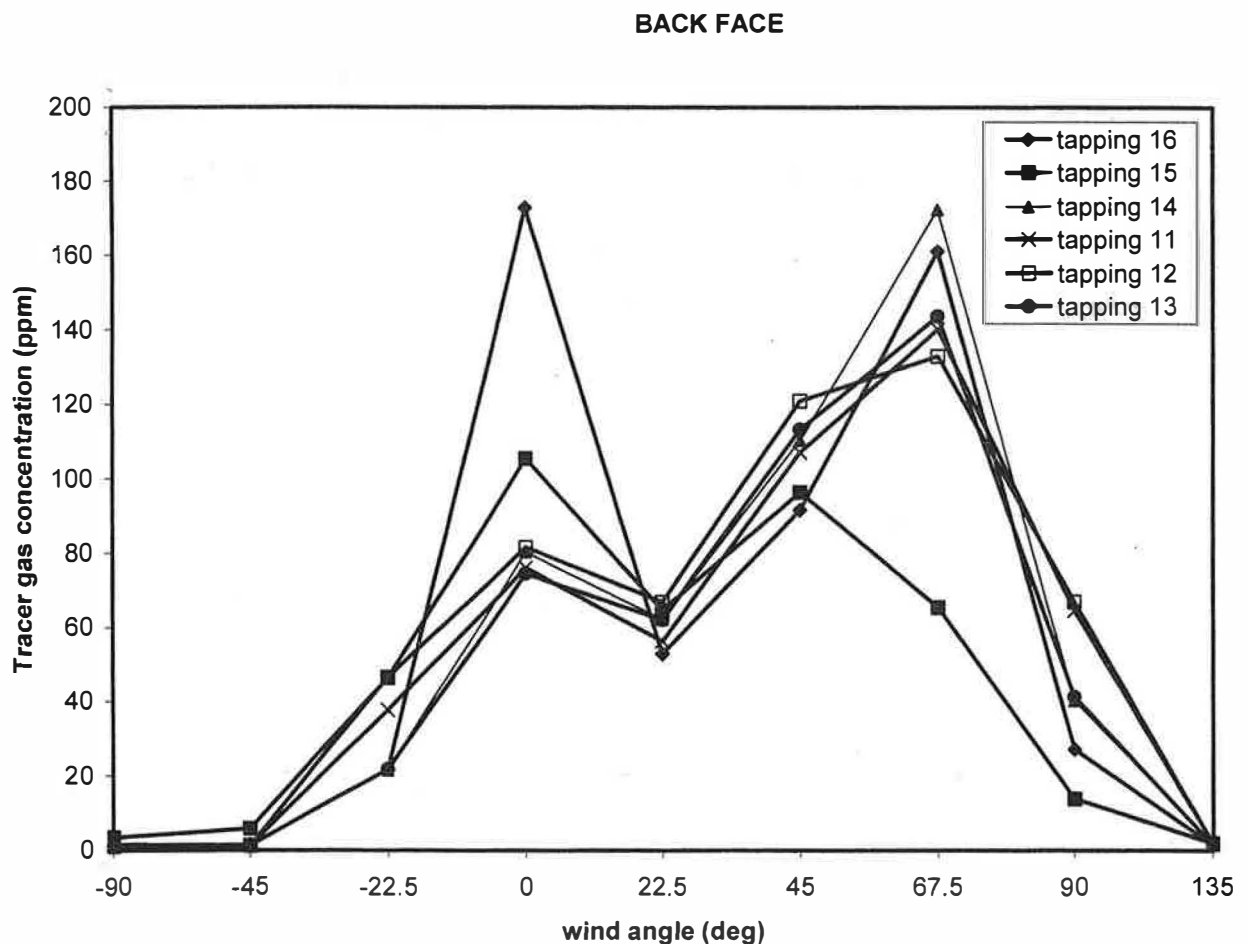


Fig. 6. Tracer gas concentrations (ppm SF₆) recorded at the backface tappings in the windtunnel. 0 deg = North wind.

SIDE 1

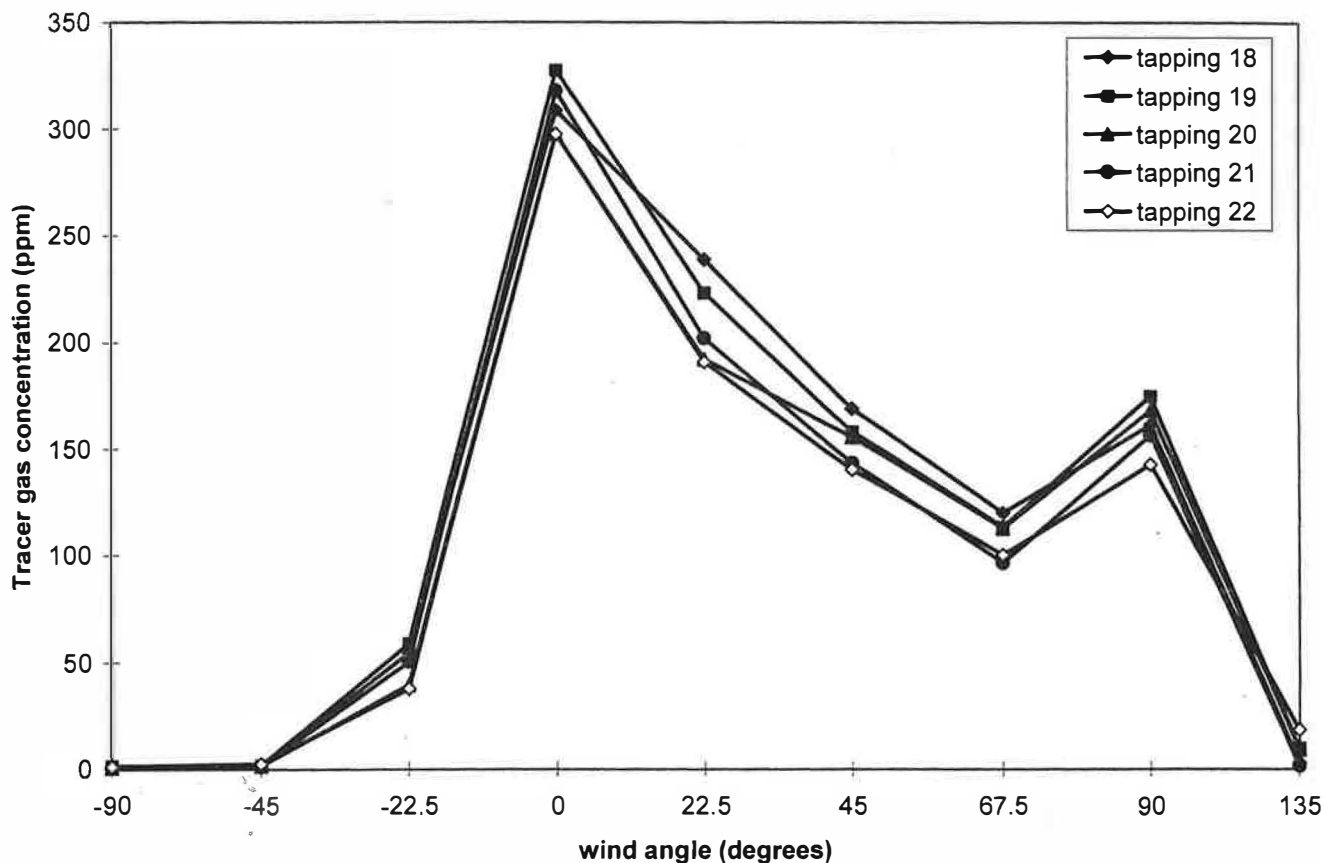


Fig. 7. Tracer gas concentrations (ppm SF₆) recorded at the side 1 tappings in the windtunnel. 0 deg = North wind.

between the kerbside sampling point and the ground floor window showed little variation in the experiments, suggesting that when averaged, the wind direction had little influence on the dilution between the points.

There are several ways of comparing the concentration readings obtained in the wind tunnel (model) and data recorded in the field (prototype) — the underlying problems are that the actual emission from the prototype vehicles in the field is unknown, and the wind direction and speed are constantly changing.

6.1. Comparison of dilutions between kerb and building

This is potentially the best comparison, because measurements at corresponding points have been made on both the prototype and the model. If we assume similarity of the velocity fields and emission characteristics, then the concentration fields should be similar, i.e.:

$$\left[\frac{C_1}{C_2} \right]_m = \left[\frac{C_1}{C_2} \right]_p \tag{3}$$

Table 4
Summary of the carbon monoxide concentrations recorded in the field study. (1) = ground floor window, (2) = first floor window

Expt	Average CO concentration (ppm)			98-percentile CO concentration (ppm)			Dilutions	
	Kerbside	Window (1)	Window (2)	Kerbside	Window (1)	Window (2)	Kerbside/Window (1)	Kerbside/Window (2)
Expt 1								
Week 1	3.91	2.32	—	14	8	—	1.75	—
Week 2	1.61	0.64	—	8	4.5	—	1.77	—
Expt 2	1.2	0.60	0.5	6.6	4.3	3.5	1.53	1.88

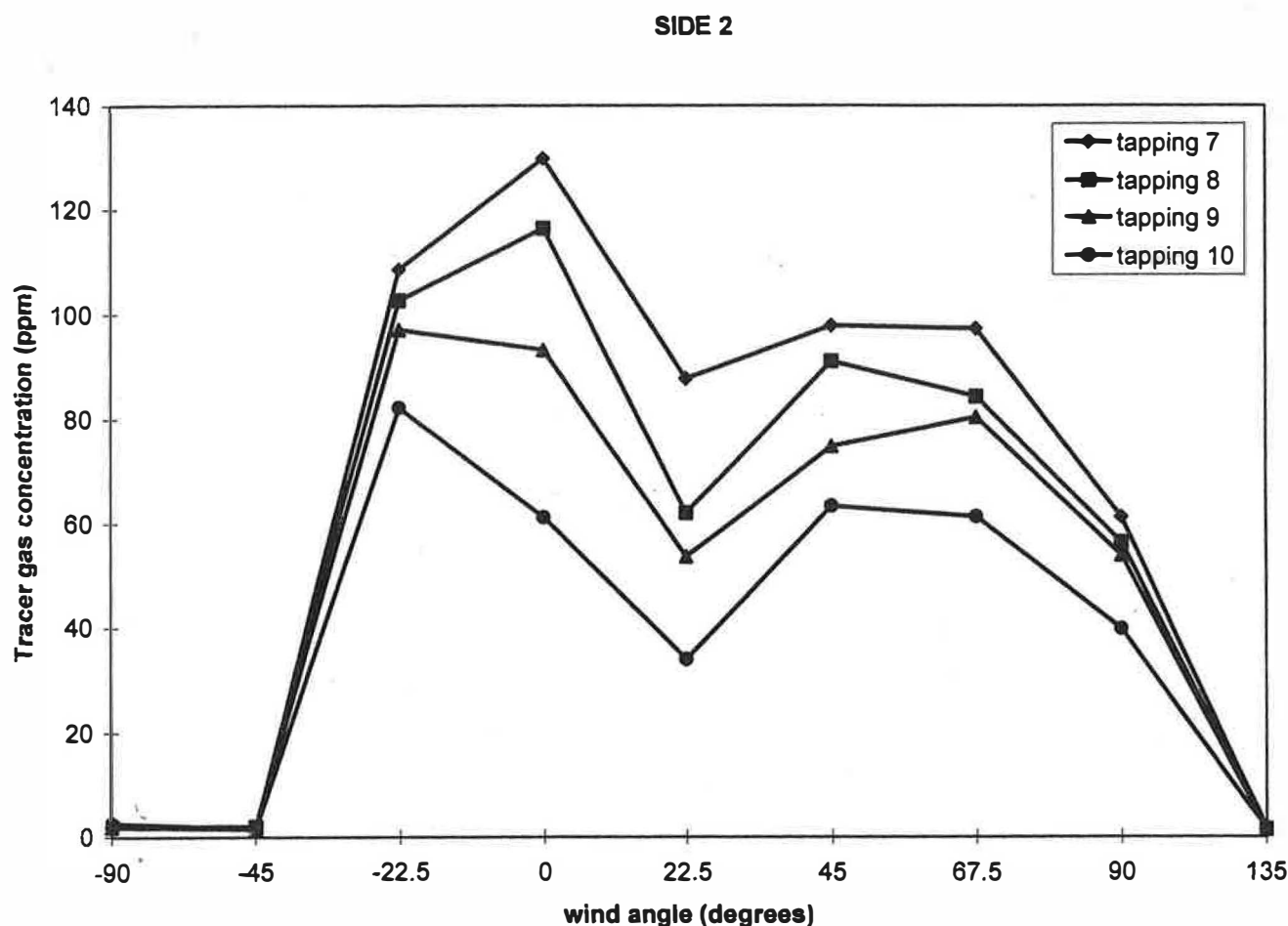


Fig. 8. Tracer gas concentrations (ppm SF₆) recorded at the side 2 tapplings in the windtunnel. 0 deg = North wind.

where the subscript m and p denote model and prototype, and C_1 and C_2 are concentrations at two specified points.

Taking $C_1 \equiv$ kerb concentration and $C_2 \equiv$ building concentration, Table 5 shows the dilutions obtained in the model for the range of wind directions measured during week 1 of Experiment 1 in the field study. During this period, the dilution between the kerbside and the ground floor window was found to be between 1.53 and 1.78, based on the 98-percentile concentrations (Table 4). The 98-percentile was used as the

basis for comparing the field and wind tunnel data in an attempt to overcome inherent difficulties in comparing the data from the two sources. By making the following assumptions, the concentrations measured in the wind tunnel can be demonstrated to be reasonably representative of those in the field.

An initial assumption, presumes that in the field study the maximum concentrations were recorded at times when the actual traffic conditions during the peak traffic periods most closely resembled the modelled queue of stationary emission points. It was also

Table 5
Dilutions measured in the wind tunnel between (i) the kerbside and tapping 2; and (ii) the kerbside and tapping 3

Wind direction	Tracer gas concentration at kerbside (ppm) [A]	Tracer gas concentration at tapping 2 (ppm) [B]	Tracer gas concentration at tapping 3 (ppm) [C]	Dilution [A]/[B]	Dilution [A]/[C]
North	1069	292	275	3.66	3.88
NN East	1643	190	160	8.67	10.26
N East	1014	125	111	8.11	9.14
EN East	967	90	66	10.74	14.65
East	783	131	114	5.93	6.89
S East	—	—	—	—	—

assumed that the maximum readings in the field were recorded when the traffic was downwind of the predominant wind direction. Hence the 98-percentile concentrations from week 1, when the wind was from a northerly to easterly direction, were compared to the wind tunnel data for the same range of wind angles.

Comparison of Tables 4 and 5 shows that the dilutions found in the wind tunnel are higher than recorded in the field, although when the wind was from the north the dilution in the wind tunnel is only greater by a factor of two. In the wind tunnel, the dilution from the kerbside to tapping 3 is marginally greater than that between the kerbside and tapping 2 — this is in accordance with observations at full scale. Considering the difference in concentration with height, Table 3 shows a 7% decrease in concentration between tappings 2 and 3. This is notably smaller than the difference in the 98-percentile concentrations observed in the field of 18%, however it is comparable to a relationship observed during rush-hour traffic. In this case it was observed that the average first floor

concentration was at times only 5% lower than that at the ground floor [17].

It is clear that the dilutions between the kerb and building are significantly larger in the wind tunnel than those observed in the field. This is unexpected to the extent that the wind tunnel does not reproduce the larger scales of turbulence which one might expect to lead to lower dilutions in the model. However, there are several factors that could account for the larger dilutions. For example, the boundary conditions at the side of the flow are not well simulated in the model; this will lead to higher dilutions in the model. However, the most likely reason lies in the simulation of the emission, which is clearly only approximate. The closer one approaches the emission line, the poorer the simulation is likely to be. Thus there could be significant errors in the kerbside values and these could have a large effect on the dilution value. One way round this problem is to compare the field and model concentrations directly, although it is necessary to make an assumption about the field emissions. This is done in

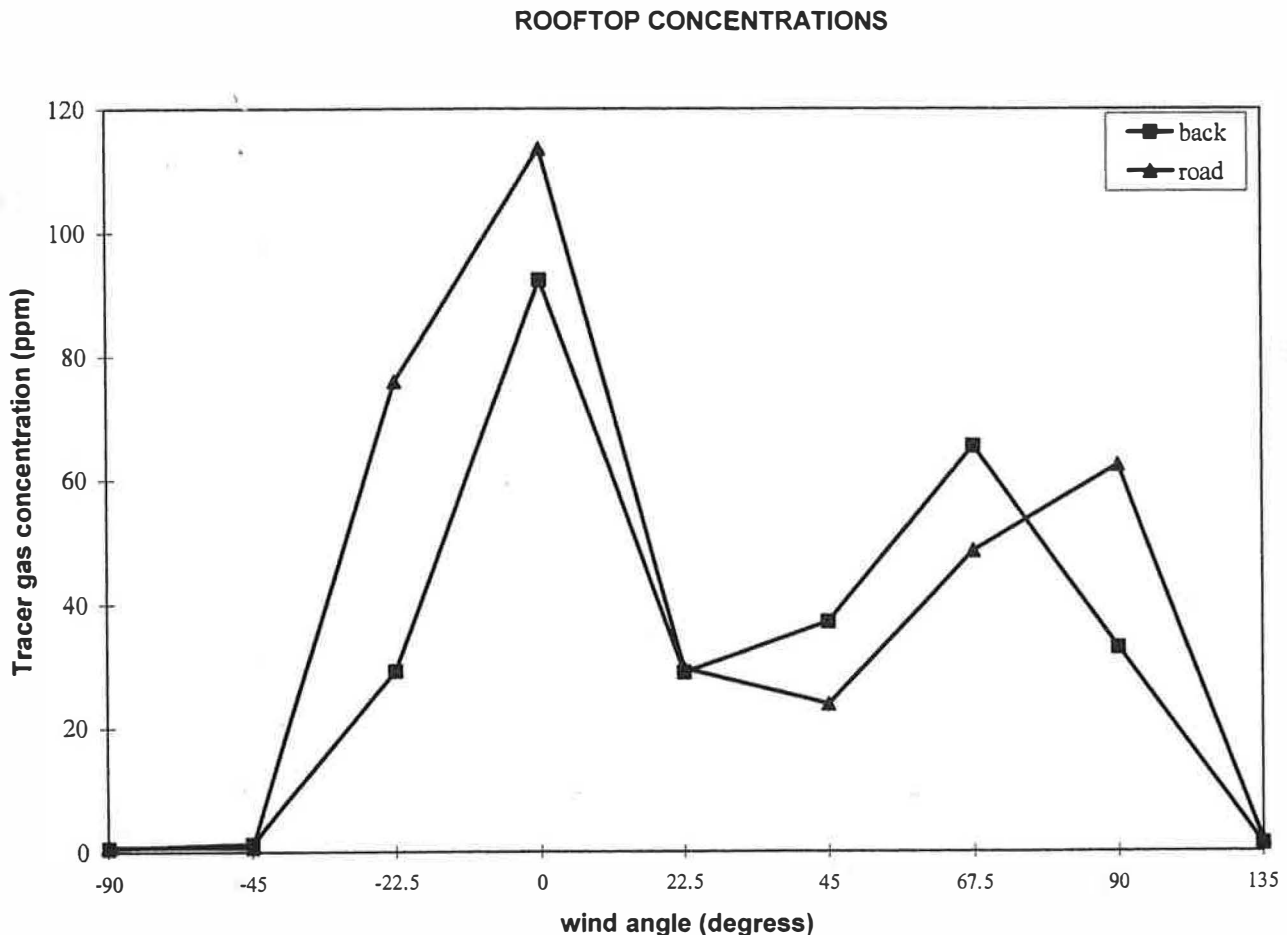


Fig. 9. Tracer gas concentrations (ppm SF₆) measured at the rooftop tappings in the windtunnel. 0 deg = North wind; back = tapping 6; road = tapping 17.

Table 6
Calculated prototype concentrations (C_p) obtained from wind tunnel data (C_m) at tappings 2 and 3

Tapping	Tracer concentration C_m (ppm SF ₆)	Concentration coefficient K_m (dimensionless)	Prototype concentration C_p (ppm CO)
2	292	2.325	7.22
3	274	2.182	6.77

the following and it will be seen that much better agreement can be obtained.

6.2. Assuming an emission value for the prototype

If similarity conditions have been adequately met then it is possible to equate the dimensionless concentration coefficients K_m and K_p , i.e.:

$$K_m = K_p \quad (4)$$

hence

$$\left[Q \frac{C}{M} \right]_m = \left[Q \frac{C}{M} \right]_p \quad (5)$$

where Q denotes a measure of the volume flow rate of air (m^3/s), C is the sampled concentration (kg/m^3) and M is the mass flow rate of the emitted gas (kg/s). K_m can be directly calculated from the wind tunnel data and if we assume a prototype emission rate and equality of K_m with K_p , then C_p can be determined. The value of C_p can then be compared to actual field results to provide a means of validating the wind tunnel data.

In the model, a line of queuing vehicles was simulated with a constant wind direction and model concentrations were compared to the 98-percentile (maximum) readings obtained in the field. It is assumed that these maximum values were recorded at periods when the traffic was at its busiest — characterised by congestion, long and short stoppages and low speeds. It is therefore difficult to assign a single emission rate (M_p) to the traffic in the prototype as the emission rate is a function of driving cycle, which is not constant over the queue length. A reasonable assumption was made that at any one time an equal proportion of the traffic would be accelerating, decelerating and idling. Thereby, using data from a similar study [22], an emission rate for CO (g/min per vehicle) was assigned to each of these driving cycles thus: accelerating 10, decelerating 8.34 and idling 3; this led to an average emission rate of 7.11 g/min per vehicle. The Appendix shows the procedure for calculating the prototype concentrations of CO in ppm from the concentration of SF₆ recorded at tappings 2 and 3 on the model for the north wind case.

The calculated prototype concentrations at tappings 2 and 3 for a northerly wind are shown in Table 6.

There is good agreement between the 98-percentile concentration at the ground floor window of 8 ppm measured in the field study (Table 4) and the prototype concentration of 7.2 ppm determined from the wind tunnel data at tapping 2. The calculated prototype concentration at the first floor window of 6.8 ppm is somewhat higher than the field measurement of 3.5 ppm, however since no wind data was available for Experiment 2 one cannot make the assumption that similar situations are being compared.

Having validated the wind tunnel data for the northerly wind, it is possible to have a degree of confidence that the relative concentrations observed in the wind tunnel are likely to be representative of those in the field under the same conditions.

7. Conclusions

The wind tunnel results have been shown to be similar to the results obtained in the field study. The comparison based on an assumed emission gives the better agreement between the field data and wind tunnel measurements, and this is most likely due to the inherent difficulties in accurately simulating the emission source. The unsteady conditions experienced in the field make direct comparison difficult, but the general relationship between the points measured in the field is consistent with wind tunnel data if some assumptions are made. Firstly, if we compare the 98-percentiles in the field data with the readings in the tunnel we are assuming that the maximum values in the field were recorded at times when the traffic was slow moving and congested, and similar to the line of static emission points in the model. Secondly, the assumption is also made that these maximum values occurred when the traffic was downwind of the predominant wind direction for the period. Neither of these assumptions is unreasonable.

The wind tunnel data indicates that the maximum concentrations on the back face may be up to 50% lower than the maximum on the roadside face. This suggests that location of air intakes on this face would offer immediate benefits to the indoor air quality. Only small reductions in concentration are found between the ground and first floor windows under traffic conditions similar to the congested flow during rush hours. However, if air intakes were situated on the

rooftop, then, irrespective of the wind direction, significantly lower concentrations of contaminants would be found here.

In addition to air intake location, a further reduction in the concentration of contaminants entering the building space could be achieved by means of ventilation control. In a previous theoretical study [23], it was illustrated how control of ventilation rates could reduce the mean indoor contaminant concentration by up to 34%. This was achieved by adjusting the ventilation rate through an opening in response to external and internal contaminant levels. Therefore, it is suggested that a combined strategy of vent location and ventilation control is most likely to yield the largest gains in terms of indoor air quality and this is the topic of current work.

Acknowledgements

The authors would like to thank the Engineering and Physical Sciences Research Council, UK, for their financial support of this project and Mr J. Stone for his assistance with the model making.

Appendix. Calculation of prototype concentration in parts per million (ppm) of CO from model measurement of SF₆ tracer gas (ppm)

If similarity conditions are satisfied then:

$K_m = K_p$ (where subscripts m and p denote model and prototype).

K is the dimensionless concentration coefficients defined by:

$$K = \frac{QC}{M}$$

where: Q is the reference volume flow rate of air; C is the sampled concentration and M is the emission rate of gas.

Q is defined by $Q = \text{wind velocity} \times \text{cross-sectional flow area}$ where cross-sectional flow area = length of emission source \times model height hence, $Q_m = 200 \times (80 \times 10) = 1.6 \times 10^5 \text{ cm}^3/\text{s}$.

At tapping 2 on the model, average concentration with north wind = 292 ppm.

Hence, $C_m = 1.453 \mu\text{g}/\text{cm}^3$

$$\text{from: } C \text{ g}/\text{cm}^3 \left[\frac{10^6}{\frac{146}{3.44E^{-5}}} \right] = C \text{ ppm}$$

where: 146 = molecular weight SF₆; $3.41 E^{-5}$ = moles of air in 1 cm³; 1 mole air = 29 l).

In the model the tracer gas SF₆ was emitted at 1 l/

min. Density of SF₆ = 6 kg/m³ hence, $M_m = 1 \times 10^5 \mu\text{g}/\text{s}$.

The above values for Q_m , C_m and M_m give $K_m = 2.325$.

An average emission factor for CO from the prototype traffic source is 7.11 g/car per min (see Section 6.2). Therefore for 40 vehicles, $M_p = 4.74 \text{ g}/\text{s}$.

$Q_p = \text{wind velocity} \times \text{length of emission source} \times \text{building height}$ (where dimensions are full scale) hence, $Q_p = 1.6 \times 10^9 \text{ cm}^3/\text{s}$.

The above values for M_p and Q_p give a value for C_p of $6.88 \times 10^{-9} \text{ g}/\text{cm}^3$.

This is equivalent to 7.22 ppm CO (with the molecular weight of CO = 28).

References

- [1] Chan CC, Özkaynak H, Spengler JD, Sheldon L. Driver exposure to volatile organic compounds, CO, ozone and NO₂ under different driving conditions. *Envir Sci Technol* 1991;25:964–72.
- [2] Chan CC, Spengler JD, Özkaynak H, Lefkopoulou M. Commuter exposure to VOCs in Boston, Massachusetts. *J Air Waste Man Ass* 1991;41:1594–600.
- [3] D.o.E. The United Kingdom national air quality strategy. Consultation Draft, 1996.
- [4] Krüger U. Location of air intakes to avoid contamination of ventilated air. In: Proc. Room Vent '94: Air Distribution in Rooms, Fourth International Conference. Krakow, Poland, 1994.
- [5] Wedding JB, Lombardi DJ, Cermak JE. A wind tunnel study of gaseous pollutants in city streets. *J Air Poll Con Assc* 1977;27(6):557–66.
- [6] Dabberdt WF, Hoydysh WG. Street canyon dispersion: sensitivity to block shape and entrainment. *Atmos Envir* 1991;25A(7):1143–53.
- [7] Hoydysh WG, Dabberdt WF. Concentration fields at urban intersections: fluid modelling studies. *Atmos Envir* 1994;28(11):1849–60.
- [8] Hüber AH. Wind tunnel and gaussian plume modelling of building wake dispersion. *Atmos Envir* 1991;25A(7):1237–49.
- [9] Mirzai MH, Harvey JK, Jones CD. Wind tunnel investigation of dispersion of pollutants due to the wind flow around a small building. *Atmos Envir* 1994;28(11):1819–26.
- [10] Bächlin W, Theurer W, Plate EJ. Wind field and dispersion in a built-up area — a comparison between field measurements and wind tunnel data. *Atmos Envir* 1991;25A(7):1135–42.
- [11] Hölsher N, Höffer R, Niemann H, Brilon W, Romberg E. Wind tunnel experiments on micro-scale dispersion of exhausts from motorways. *Sci Total Envir* 1993;134:71–9.
- [12] Kraenzmer M. Modelling the influence of outdoor pollutants on the indoor air quality in buildings with air flow rate control. In: Proceedings of the Seventeenth AIVC conference, Gothenburg, Sweden 1996, 1996.
- [13] Ajiboye P, Hesketh M, Willan P. The significance of urban pollution and its dilution associated with height. In: Proceedings of the Eighteenth AIVC Conference, Athens, Greece, 1997, 1997.
- [14] Trepte L. Ventilation strategies in the case of polluted outdoor air situations. In: Proceedings of Effective Ventilation, Ninth AIVC Conference, Gent, Belgium, 1988, 1988.
- [15] Ekberg LE. Relationship between indoor and outdoor contami-

- nants in mechanically ventilated buildings. *Indoor Air* 1996;6:41–7.
- [16] Ratcliff MA, Petersen RL, Cochran BC. Wind tunnel modelling of diesel odors for fresh-air-intake design. Preprint for inclusion in ASHRAE Trans 1994;100(2).
- [17] Green NE, Riffat SB, Etheridge DW, Clarke R. Traffic pollution in and around a naturally ventilated building. *Building Services Engineering Research and Technology* 1998;19(2):67–72.
- [18] Sexton DE. A simple wind tunnel for studying air flow around buildings. BRE current paper, 1968.
- [19] Tieleman HW. Problems associated with modelling procedures for low-rise structures. *J Wind Eng Ind Aerodyn* 1992;41(44):923–34.
- [20] Etheridge DW, Stanway RJ. Application of the constant concentration technique for measurement in large buildings. In: Talk presented to SERC Workshop on Ventilation. 25–26 Oct. 1984, Coventry Polytechnic, 1995.
- [21] Engineering Sciences Data Unit. Characteristics of atmospheric turbulence near the ground. 75001, ESDU, London, 1975.
- [22] Mataoro A. Results from a model of road traffic air pollution, featuring junction effects and vehicle operating modes. *Traffic Engineering & Control*, Jan 1990.
- [23] Green NE, Riffat SB, Etheridge DW. Ventilation control: its effect on indoor concentrations of traffic pollutants. *Building Services Engineering Research and Technology* 1998;19(3):149–54.